Supplementary Information

Kilometer-scale global warming simulations and active sensors reveal changes in tropical deep convection

Maximilien Bolot[1], Lucas Harris[2], Kai-Yuan Cheng[1]
Timothy M. Merlis[1], Peter Blossey[3], Christopher Bretherton[4]
Spencer K. Clark[2,4], Alex Kaltenbaugh[2,5], Linjiong Zhou[1,2]
and Stephan Fueglistaler[1]

[1]Program in Atmospheric and Oceanic Sciences, Princeton University, NJ, USA
[2]NOAA/Geophysical Fluid Dynamics Laboratory, Princeton, NJ, USA
[3]Atmospheric Sciences, University of Washington, Seattle, WA, USA
[4]Allen Institute for Artificial Intelligence, Seattle, WA, USA
[5]University Corporation for Atmospheric Research, Boulder, CO, USA

November 6, 2023

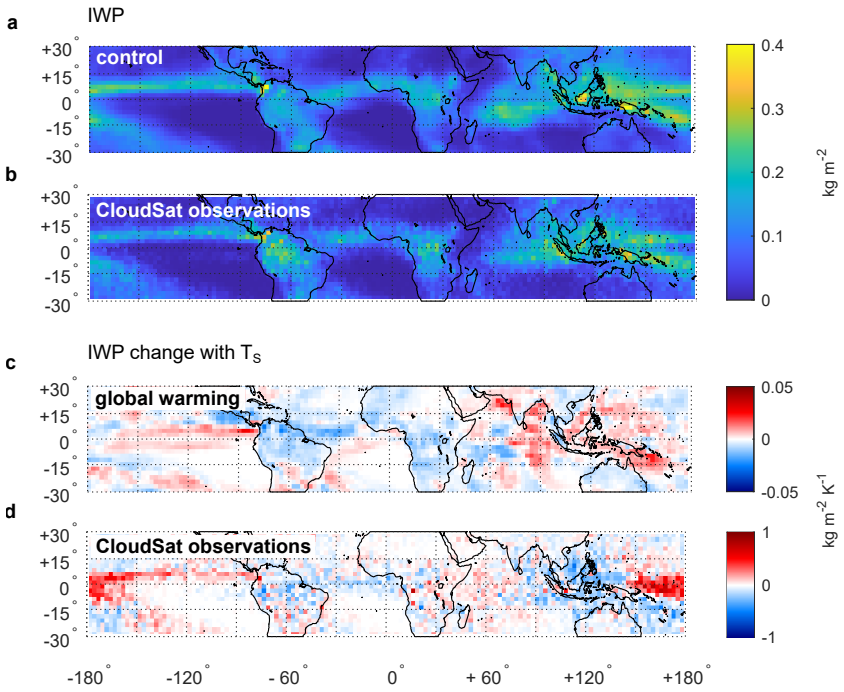

Supplementary Figure 1: Geographic distribution of IWP and response with uniform warming in the global warming experiment of X-SHiELD and with interannual temperature variations in CloudSat observations (2B-CWC-RO), computed on a regular grid at 2.5° resolution. Time-averaged geographic distribution of IWP in (**a**) the control simulation and (**b**) CloudSat observations (from July 2006 to December 2010). Change of IWP per tropical-mean T_S in (**c**) the global warming experiment and (**d**) CloudSat observations. In (**d**), the values are from a regression of IWP interannual anomalies against T_S interannual anomalies (derived from ERA5). Tropical-mean T_S is defined from 20°S to 20°N.

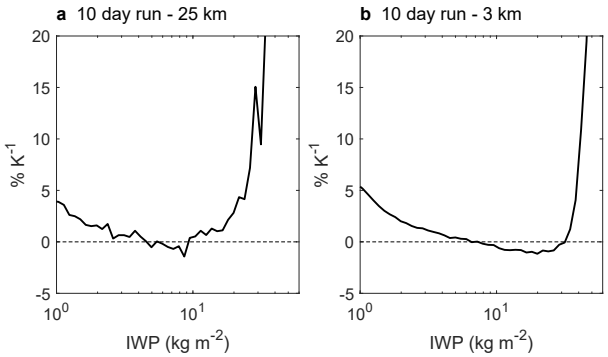

Supplementary Figure 2: Change in the frequencies of IWP in short (10 days, from the 1st to the 10th of August) simulations of the global warming GSRM experiment (**a**) in the 25 km output of the 3 km model and (**b**) in the 3 km output of the 3 km model. Note that the runs are short and not fully equilibrated. Thus, Supplementary Fig. 2a should not be compared to Fig. 1d of the main text.

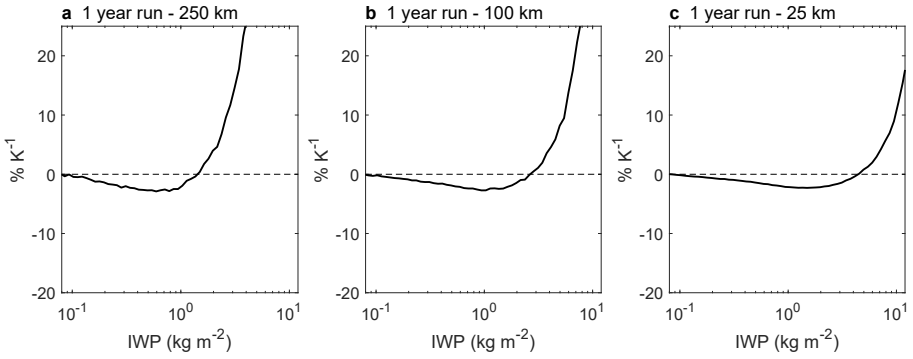

Supplementary Figure 3: Change in the frequencies of IWP in the year-long simulations of the global warming GSRM experiment (**a**) in the 250 km output of the 3 km model, (**b**) in the 100 km output of the 3 km model and (**c**) in the 25 km output of the 3 km model (same as Fig. 1d of the main text).

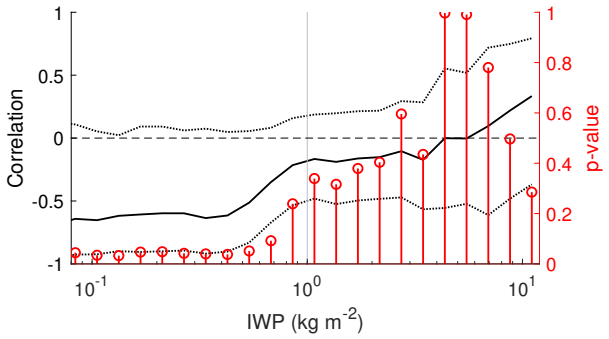

Supplementary Figure 4: Correlations of the interannual anomalies of IWP frequency in the CloudSat observations (2B-CWC-RO) with interannual anomalies of tropical-mean surface temperature T_S (solid line), with the 95 % confidence interval on the correlations (dashed lines) and the corresponding p-values (probability of observing a correlation as extreme if the true correlation were zero). The CloudSat observations are the same as in Fig. 1 of the main text (2B-CWC-RO, from 2006 to 2010). See Methods for more information.

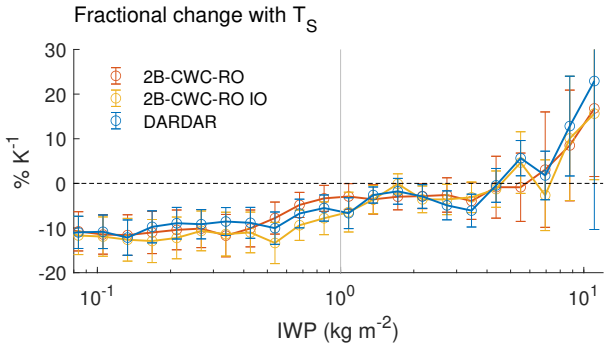

Supplementary Figure 5: Comparison of IWP frequency change with interannual surface temperature variations T_S in the tropics in the Level 2B Radar-only Cloud Water Content product (2B-CWC-RO), the Level 2B Radar-only Cloud Water Content product assuming ice only retrieval (2B-CWC-RO IO) and the raDAR/liDAR ice cloud property retrieval product (DARDAR). The period of the observations is from July 2006 to December 2010. The error bars indicate the standard errors of regression of the IWP interannual frequency anomalies on the T_S interannual anomalies.

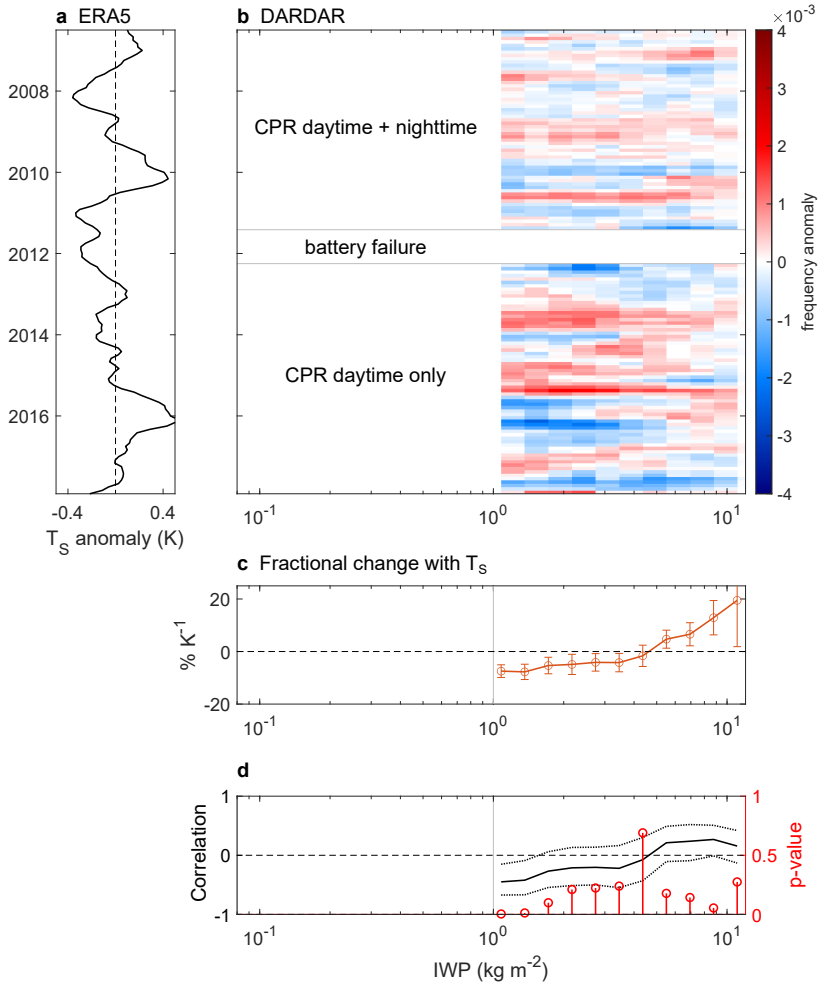

Supplementary Figure 6: Change in the frequencies of IWP with interannual temperature variations in DARDAR observations of active convection (IWP > 1 kg m^{-2}) from July 2006 to December 2017. (**a**) Interannual anomalies of tropical-mean surface temperature T_S in the ERA5 reanalysis. (**b**) Interannual anomalies of IWP frequency in DARDAR observations, with the operational status of the cloud physics radar (CPR) of CloudSat reported in the panel. (**c**) Fractional change of IWP frequency per T_S warming. The error bars indicate the standard errors of regression of the IWP interannual frequency anomalies on T_S interannual anomalies. (**d**) Correlation of the IWP interannual frequency anomalies with T_S interannual anomalies (solid line), with the 95 % confidence interval on the correlations (dashed lines) and the corresponding p-values (probability of observing a correlation as extreme if the true correlation were zero). See Methods for more information.

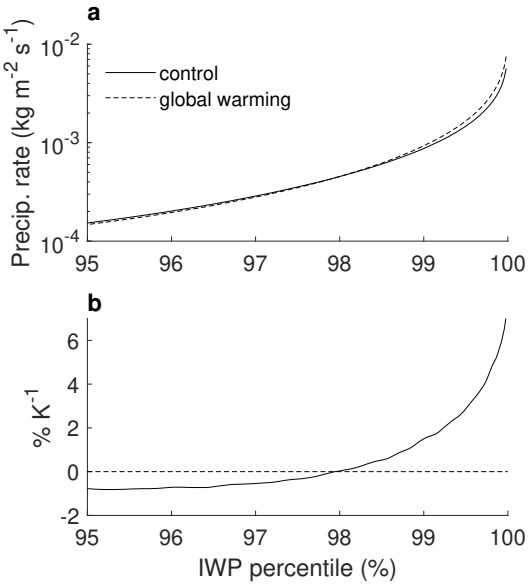

Supplementary Figure 7: Response of surface precipitation rate at fixed IWP percentile in the global warming GSRM experiment. (**a**) Precipitation rate in present-day climate (control) and in the warmer future climate. (**b**) Fractional increase of the precipitation rate with tropical-mean T_{S} at constant percentile.